Thermosetting Cure Diagrams: Calculation and Application

S. L. SIMON and J. K. GILLHAM*

Polymer Materials Program, Department of Chemical Engineering, Princeton University, Princeton, New Jersey 08544

SYNOPSIS

The time–temperature–transformation (TTT) isothermal cure diagram and the continuous-heating-transformation (CHT) cure diagram are calculated from a reaction model for a high-T_g epoxy/amine system that has been developed to describe both epoxy/amine and etherification reactions in kinetically and diffusion-controlled reaction regimes. The cure diagrams are applied to various processing operations. The optimization of processing and of material properties by exploiting gelation and/or vitrification during cure is discussed.

INTRODUCTION

The time–temperature–transformation (TTT) isothermal cure diagram, adapted to thermosetting polymers[1,2] and shown in Figure 1, provides an intellectual framework for understanding the curing process. During cure to full conversion, the glass transition temperature (T_g) increases from the value for the uncured monomer mixture (T_{g0}) to the "fully cured" value ($T_{g\infty}$). When the isothermal cure temperature, T_c, is much lower than $T_{g\infty}$, the reaction generally becomes diffusion-controlled as T_g increases through T_c and a limiting value of T_g, which depends on T_c, is obtained. Gelation and vitrification are the two principal transformations that may occur during cure: Molecular gelation is the incipient formation of infinite molecules that occurs in the simplest systems at a fixed conversion and a T_g of ${}_{gel}T_g$; vitrification is solidification that is defined to occur when T_g reaches T_c. The continuous-heating-transformation (CHT) cure diagram is similar to the TTT isothermal cure diagram but displays the time to transformations that occur during the course of continuous heating at different heating rates.[3–5] Since gelation and vitrification control the rheology, reaction rate, density, dimensional stability, internal stresses, and, in fact, all properties of a thermosetting material, these transformations can be exploited during cure to optimize processing and final material properties. To that end, the TTT and CHT cure diagrams are used in this article to design time/temperature cure paths for various processing operations. Although the cure diagrams can be obtained, in principle, directly from experiments, their quantitative exploitation requires development of a reaction model.

Previous work in our laboratory modeled the kinetics and calculated the TTT isothermal cure diagram and the CHT cure diagram for the stoichiometric ratio (1 : 1) of an aromatic difunctional epoxy/aromatic tetrafunctional diamine system in both the kinetically and diffusion-controlled regimes using T_g as the primary variable.[5,6] In the present work, the model presented has been modified by incorporation of the etherification reaction to describe the cure of both an amine-rich mixture and an epoxy-rich mixture, again using T_g as the primary variable. Off-stoichiometric mixtures are used in order to further test the model and also because properties after cure may be optimized by using off-stoichiometric mixtures[7] (e.g., $T_{g\infty}$ is actually higher for the epoxy-rich system studied in this work than for the 1 : 1 system). TTT isothermal cure and CHT cure diagrams are calculated for both of the off-stoichiometric epoxy/amine systems using the model of the reaction. More complete reports on the reaction model are available.[8,9] Application of the diagrams to various processes in order to optimize the processes or the final material properties is discussed.

* To whom correspondence should be addressed.

Journal of Applied Polymer Science, Vol. 53, 709–727 (1994)
 CCC 0021-8995/94/060709-19

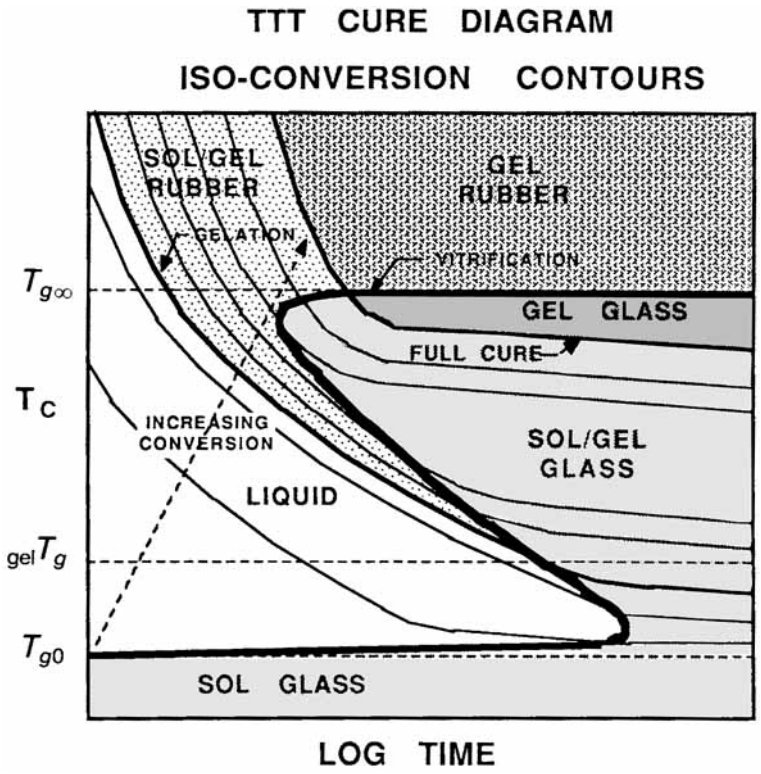

Figure 1 Generalized TTT isothermal cure diagram with iso-T_g contours. Gelation, vitrification, and iso-T_g (= isoconversion) contours are shown, as are the various states of the material.

MATERIALS

The chemical system used is a liquid difunctional epoxy, a diglycidyl ether of bisphenol A (DER 332, Dow Chemical Co.: 174 g/equiv; theoretical 170 g/equiv), cured with a crystalline tetrafunctional aromatic diamine, trimethylene glycol di-*p*-aminobenzoate (TMAB, Air Products Corp., 78.5 g/equiv, melting point = 125°C). The chemical structures of the reacting materials are shown in Figure 2. Two off-stoichiometric ratios of the reactants are studied: an excess amine mixture (1 : 1.2 epoxy groups to amino hydrogen atoms) and an excess epoxy mixture (1 : 0.8 epoxy groups to amino hydrogen atoms). Samples were mixed at 100°C until the solutions became clear and homogeneous. The mixtures were stored in a freezer until needed (≈ -15°C). Minimal reaction occurs during the initial mixing process.[8,9] The glass transition temperatures of the uncured mixtures, T_{g0}, are -4 ± 1 and -9 ± 1°C for the amine-rich and epoxy-rich stoichiometries, respectively, as compared to a value of -5°C reported for the 1 : 1 mixture.[6]

EXPERIMENTAL

All experimental data reported in this work were obtained from differential scanning calorimetry (DSC) studies using a Perkin-Elmer DSC-4 unit. Ten to fifteen milligram samples of uncured resin were sealed in aluminum DSC pans. A simple DSC temperature scanning experiment from -30 to 350°C at 10°C/min yields the T_g and the exothermic residual heat of the epoxy/amine reactions for both epoxy-rich and amine-rich samples. To obtain the conversion of the etherification reaction in the epoxy-rich samples, a second type of DSC experiment was performed since a simple temperature scan is complicated by thermal degradation at the high temperatures[8,9]: A temperature scan from -30 to 320°C at 10°C/min yields the T_g and the exothermic residual heat of the epoxy/amine reactions and then an isothermal hold at 320°C for 60 min yields the residual heat of the excess epoxy reactions. Samples were cured for various cure times, t, ranging from 10 min to 24 h, in the preheated DSC unit at isothermal cure temperatures, T_c, from 100 to 200°C

CHEMICAL REACTANTS

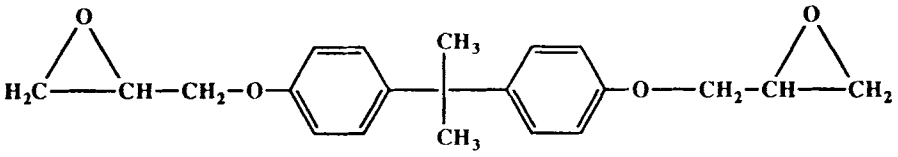

Diglycidyl Ether of Bis-phenol A

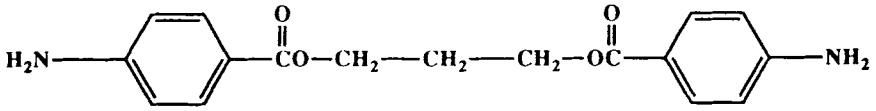

Trimethylene Glycol Di-p-aminobenzoate

Figure 2 Chemical structures of the reactants.

and cooled at 10°C/min to −30°C prior to the DSC temperature scanning experiment. Samples cured for cure times ranging from 1 to 7 days were cured in an oven at isothermal cure temperatures from 100 to 200°C, allowed to free cool to room temperature, and then quenched in the DSC unit from room temperature to −30°C prior to the temperature scanning experiment. Samples that vitrified during cure ($T_g > T_c$) had the effects of physical aging on T_g removed by stopping the DSC temperature scanning experiment immediately after the endothermic relaxation at T_g, quenching at 320°C/min to −30°C, and then rescanning to obtain the unaged T_g and the exothermic residual heat(s) of reaction.[6,8,9] No discrepancies were observed between samples cured in the DSC unit and samples cured in the oven or between those that did or did not vitrify during cure.

The fractional conversion of epoxy, x, for the amine-rich system is determined assuming that only epoxy/amine reactions occur and that all of the epoxy can react:

$$x = 1 - \frac{\Delta H_{r1}}{\Delta H_{T1}} \qquad (1)$$

where ΔH_{r1} and ΔH_{T1} are the residual heat and total heat (−102 ± 8 kJ/mol of epoxy) of the epoxy/amine reactions, respectively. The fractional conversion of epoxy for the epoxy-rich system is due to both the epoxy/amine reactions and the reactions of excess epoxy. Assuming that the stoichiometric amount of epoxy reacts with amine with the excess reacting via etherification,

$$x = 1 - 0.8\frac{\Delta H_{r1}}{\Delta H_{T1}} - 0.2\frac{\Delta H_{r2}}{\Delta H_{T2}} \qquad (2)$$

where the subscript 2 refers to the reaction of excess epoxy, with ΔH_{T2} being approximately −84 ± 13 kJ/mol of reacting epoxy, 20% less than the total heat for the epoxy/amine reactions (ΔH_{T1}) as observed by other researchers.[10]

REACTION MODEL AND CALCULATION OF CURE DIAGRAMS

Chemical Kinetics

Three principal reactions occur in epoxy/amine systems: the stepgrowth reactions of epoxy with primary and secondary amines catalyzed by hydroxyl, and the much slower polymerization reaction of epoxy with hydroxyl generated from the epoxy/amine reactions catalyzed by base:

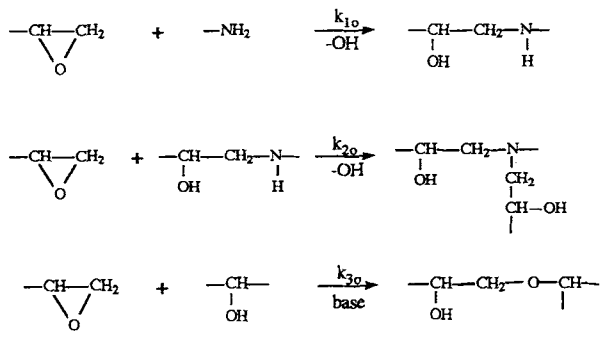

where k_{10}, k_{20}, and k_{30} are the rate constants. Due to the high concentration of hydroxyl relative to the epoxy in the later stages of cure when the reaction between epoxy and hydroxyl is significant (see later), this reaction is considered to terminate at the first step, resulting in etherification, rather than in polyetherification.

The stoichiometric reaction of the epoxy/amine system investigated has been satisfactorily described by a second-order mechanism for the epoxy/amine reactions autocatalyzed by hydroxyl groups generated during the reaction assuming equal reactivities of amino hydrogens.[6] The same model has been used to describe the off-stoichiometric systems but with the added complexity of the etherification reaction and a consideration of unequal reactivities of amino hydrogens.[8,9] The reaction model is described in this work since it will be used as an example to calculate the TTT and CHT cure diagrams, which are then applied to various processing applications.

The epoxy/amine reactions are assumed to be first order with respect to epoxy, amine, and hydroxyl concentrations.[11] Etherification is assumed to be first order with respect to both epoxy and hydroxyl concentrations and is not considered to be catalyzed by tertiary amine due to steric hindrance as in the work of other researchers.[12] Note, however, that if etherification were catalyzed by tertiary amine, the concentration could be implicitly incorporated into the rate constant since it is constant when the reaction becomes significant. The change with time of epoxide and primary amine fractional conversions, x and x_1, respectively, can be described by the following differential equations:

$$\frac{dx}{dt} = k_1(1-x)(x+b)(1-x_1) + k_2(1-x)(x+b)x_2 + k_3(1-x)x$$
$$= k_1(1-x)(x+b)(1-x_1+\alpha x_2) + k_3(1-x)x \quad (3)$$

$$\frac{dx_1}{dt} = k_1 r(1-x)(x+b)(1-x_1) \quad (4)$$

where x_2 is the yield of tertiary amine and is related to x and x_1.[8,9] The first two terms on the right-hand side of eq. (3) describe the reaction of epoxy with primary and secondary amines, respectively, whereas the third term describes the reaction of epoxy with hydroxyl. The stoichiometric ratio, r, is e_0/a_{10}, where e_0 and a_{10} are the initial concentrations of epoxy and primary amine, respectively. The parameters in the equations are determined by fitting the experimental DSC data.[8,9] The rate constants are normalized Arrhenius rate constants, having units of time^{-1}: $k_1 = k_{10}e_0a_{10}$ and $k_3 = k_{30}e_0$. At 150°C, $k_1 = 0.37$ min^{-1}. The dimensionless ratio of the normalized rate constants for the reactions of epoxy with secondary and with primary amine groups, $\alpha = k_2/k_1$, is found to be 0.5, indicating equal reactivities of amino hydrogens, within the range of 0.1–0.5 observed by other researchers using various methods.[12–17] The dimensionless ratio of the normalized rate constants for the reactions of epoxy with hydroxyl and primary amine groups, $\beta = k_3/k_1$, is found to be 0.001. The low value of β results in the etherification reaction being significant only in the epoxy-rich system and then only after essentially all amino hydrogens have been depleted, in agreement with other researchers.[12,14,15,18,19] The constant b is considered to be the concentration of initial hydroxyl or impurities that catalyze the reaction and is particularly significant at low conversions.[11] The values of b are 0.05 and 0.10 for the epoxy-rich and amine-rich systems, respectively, with the difference being attributed to more prereaction in the amine-rich system due to the longer time of mixing (30 vs. 15 min at 100°C). The activation energies for the epoxy/amine and etherification reactions appear to be identical at 15.5 kcal/mol from time–temperature superposition of conversion vs. log time data.[8,9]

Diffusion control becomes important for the reactions in the vicinity of vitrification, $T_g = T_c$, and must be incorporated into the reaction model. Similar to other work in this area,[6,20,21] diffusion control in this work is accounted for by assuming that the time scale for the disappearance of a reactant ($1/k_i$, where i is 1 or 3) is equal to the time scale for chemical reaction in the absence of diffusion ($1/k_c$) plus the time scale for diffusion ($1/k_d$):

$$\frac{1}{k_i} = \frac{1}{k_c} + \frac{1}{k_d} \quad (5)$$

The time scale for diffusion is considered to depend on the fractional free volume in the Doolittle equation[22] due to its simplicity and the satisfactory results:

$$k_d = A \exp(-b_d/f) \quad (6)$$

where A and b_d are taken as adjustable parameters and are found to be $A = 100$ and 0.4 for the epoxy/amine (k_1) and etherification reactions (k_3), respectively, with $b_d = 0.2$ for both stoichiometries. The lower value of A for the etherification reaction indicates a lower mobility due presumably to the higher cross-link density in the later stages of cure when this reaction is significant. The fractional free volume f is assumed to be the equilibrium value as calculated using the "universal" values found for various polymers from the William–Landel–Ferry (WLF) equation[23]:

$$f = (T_c - T_g)(4.8 \times 10^{-4}) + 0.025 \quad (7)$$

Use of the above equilibrium equation is a good first approximation since the material never enters the glassy state for the time scales studied, but, rather, always cures in the rubbery or glass transition regimes with $T_g \leq T_c + 30°C$ (assuming the glass transition is 60°C wide).

The above reaction model describes the conversion as a function of time, temperature, and T_g in both kinetically and diffusion-controlled reaction regimes in the absence thermal degradation (which occurs at temperatures above 200°C[8,9]). By using an additional relationship between conversion and T_g, the model describes T_g as a function of time and temperature. In this work, the experimental T_g vs. time data at various isothermal temperatures will be compared with the calculated results using the relationship between T_g and conversion.

T_g vs. Conversion

A one-to-one relationship between T_g and conversion is found for the amine-rich system and is independent of cure temperature for the cure temperatures studied, as shown in Figure 3. Similar results are found for various stoichiometric epoxy/amine systems.[5,10,24–27] For the epoxy-rich system, the T_g vs. conversion relationship shown in Figure 4 is also unique and independent of cure temperature for conversions below 0.8 where the primary reaction is epoxy with amine. Data at higher conversions show more scatter, and, consequently, the uniqueness of the relationship in this regime is not proved although it is expected since the activation energies

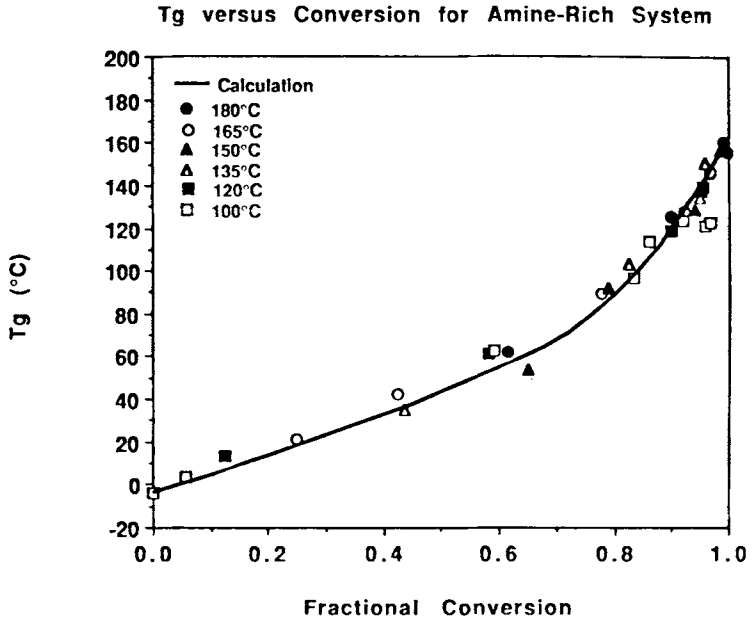

Figure 3 T_g vs. conversion for the amine-rich system showing the one-to-one relationship independent of cure temperature. Symbols are experimental data; the solid curve is the calculated relationship.

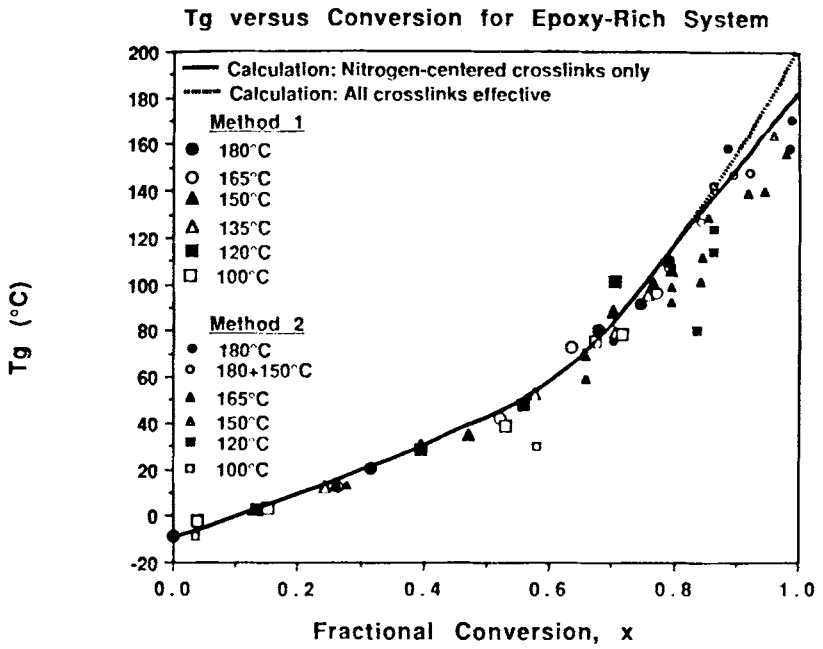

Figure 4 T_g vs. conversion for the epoxy-rich system showing the one-to-one relationship independent of cure temperature. Symbols are experimental data; the solid and dotted lines are the calculated relationships assuming that only amine-centered or that all cross-links are effective in raising T_g, respectively.

of the various reactions are found to be similar and the epoxy/amine and etherification reactions are found to be sequential. The one-to-one relationship between T_g and conversion is important because T_g is a more accurate and sensitive parameter for monitoring the reaction than is fractional conversion calculated from the residual heat of reaction.[6,24] T_g is also directly related to the solidification process. The one-to-one relationship between T_g and conversion implies that either the molecular structure of the materials cured at different cure temperatures is the same (i.e., the competing reactions have similar activation energies, as is considered the case) or that the difference in molecular structure for materials cured at different temperatures does not have a significant effect on the glass transition temperature (i.e., the differences in structure occur on a sizescale smaller than that measured by T_g).

The T_g vs. conversion data are fit by an adaptation of a recently published equation that is based on the DiMarzio equation[28] and that relates T_g to the conversion and cross-link density of the material[10]:

$$T_g(x) = \frac{1}{\left(\frac{1}{T_{g0}} - kx\right)\left(1 - \frac{KX}{(1 - \Psi X^2)}\right)} \quad (8)$$

where x is the fractional conversion of epoxy. The variable X is taken as the effective cross-link density of trifunctional cross-links in this work, since in the epoxy-rich system, two types of trifunctional cross-links are formed that may not be equally effective in raising T_g: The reaction of epoxy with amine results in the typical nitrogen-centered (amine) cross-links, whereas the etherification reaction may result in a carbon-centered cross-link and an amine cross-link. The cross-link density due to each type of cross-link is determined[8,9] as a function of conversion using the recursive theory,[29] which assumes that no intramolecular reactions occur prior to gelation. The parameters k, K, and Ψ reflect the effects on T_g of chain ends, cross-links, and the non-Gaussian nature of the segments between cross-links, respectively. The calculated curves are shown in Figures 3 and 4, using $k = 0.00175e_0$, $K = 0.24$, and $\Psi = 0.0$, where e_0 is the initial concentration of epoxide in moles per total moles reactants.[8,9] In the epoxy-rich system, two curves are plotted for the two extreme cases: one in which all cross-links are considered equally effective, and the other in which only nitrogen-centered (amine) cross-links are considered effective. The data are better predicted in the latter case in which only nitrogen-centered cross-links are considered effective at raising the T_g. The use of the

theoretical equation reduces the effect of scatter in the residual heat data, especially at high conversions for the epoxy-rich system, and will be used to transform conversion to T_g when using the reaction model to calculate T_g as a function of time and temperature. Consequently, the T_g vs. conversion relationship described by eq. (8) will be used in the reaction model. However, an empirical fit of the experimental data could alternately be used in the model.

Calculation of T_g vs. Time

The calculated T_g vs. ln time curves (solid lines) satisfactorily fit the experimental data in Figures 5 and 6 for isothermal cure temperatures from 100 to 200°C. In the amine-rich system, the data level off at $T_{g\infty}$ ($\approx$ 160°C) for high cure temperatures due to full conversion of epoxy in the absence of degradation reactions. In the epoxy-rich system, T_g begins to level off upon full conversion of the amine at $T_{g\infty 1}$ ($\approx$ 120°C) and, then, subsequently increases to $T_{g\infty 2}$ ($\approx$ 180°C) upon full conversion of the epoxy. The model also satisfactorily fits the experimental data of the 1 : 1 stoichiometric system,[8,9] as would be expected.

The reaction model with diffusion control incorporated [eq. (3)-(7)] can be used not only to calculate the conversion (or T_g using the relationship between T_g and conversion) as a function of time for an isothermal cure as shown in Figures 5 and 6, but also for calculating time–temperature–transformation (TTT) isothermal cure diagrams and the continuous-heating-transformation (CHT) cure diagrams. Procedures for calculating the TTT and CHT cure diagrams have been described.[5,6,30] These diagrams can be then used to design time/temperature cure paths that exploit gelation and/or vitrification in order to optimize processing or final material properties for various processing operations.

Time–Temperature–Transformation (TTT) Isothermal Cure Diagrams

Figures 7 and 8 show the calculated TTT isothermal cure diagrams for the two off-stoichiometric systems. The diagram is calculated by numerical integration of the reaction model to yield the conversion and T_g vs. time at various cure temperatures. Utilizing the results of the integration, the times to gelation ($T_g = {}_{gel}T_g$) and vitrification ($T_g = T_c$) are plotted as a function of cure temperature on the diagram and result in the gelation and vitrification contours, respectively. The iso-T_g contours (every 20°C from T_g = 0°C to $T_{g\infty}$) are similarly plotted on the diagram. The gelation curves correspond to iso-T_g (isoconversion) contours: Gelation occurs at the incipient formation of infinite molecules that would occur in

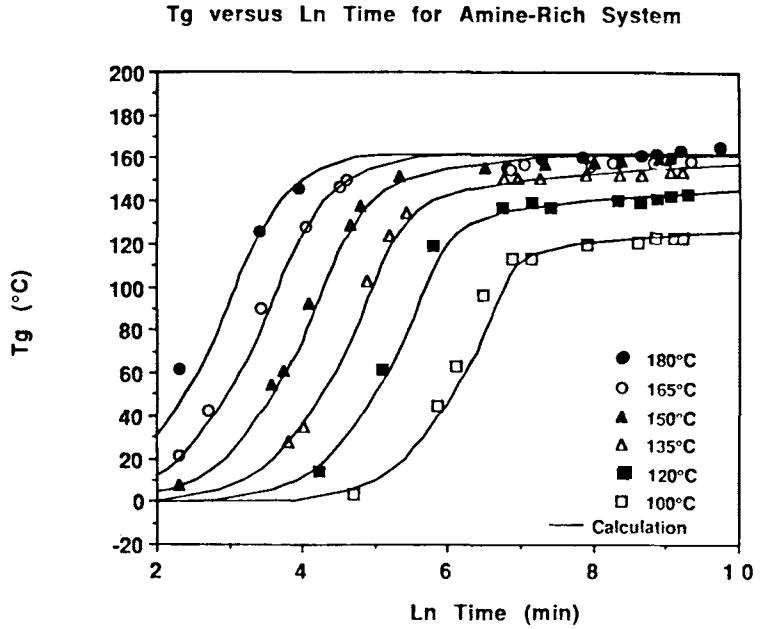

Figure 5 T_g vs. ln time for the amine-rich system. Symbols are experimental data; solid curves are calculations from the reaction model.

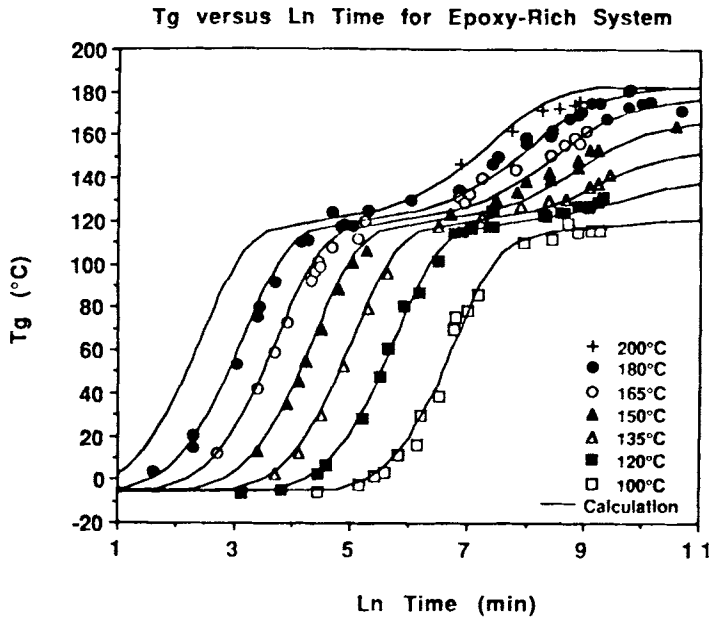

Figure 6 T_g vs. ln time for the epoxy-rich system. Symbols are experimental data; solid curves are calculations from the reaction model.

the absence of intramolecular reactions[31] at theoretical epoxide fractional conversions of 0.65 and 0.53 (corresponding to T_g's of 69 and 46°C) for the epoxy-rich and amine-rich systems, respectively. There is a noticeable difference in the shapes of the vitrification curves for the two off-stoichiometric mixtures. The vitrification curve of the amine-rich system levels off at cure temperatures close to its $T_{g\infty}$, as expected, due to full conversion of the epoxy, whereas the vitrification curve for the excess epoxy

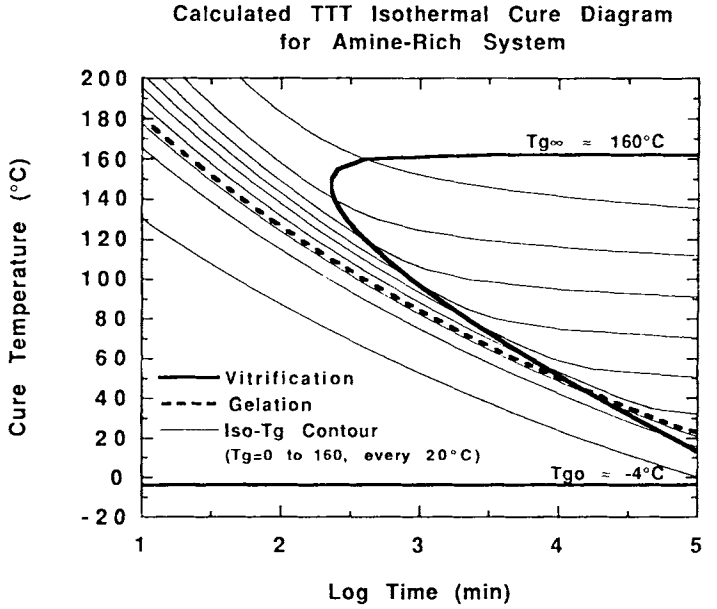

Figure 7 Calculated TTT isothermal cure diagram for the amine-rich system, showing gelation, vitrification, and iso-T_g (every 20°C from 0 to $T_{g\infty}$) contours.

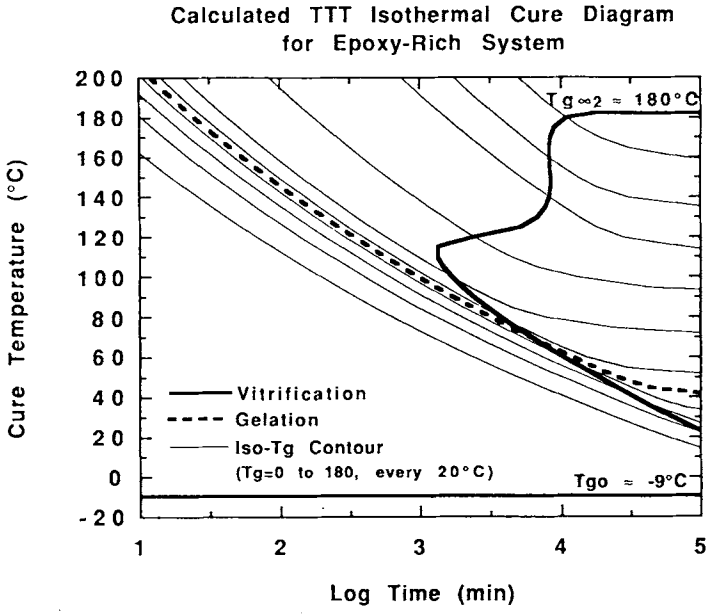

Figure 8 Calculated TTT isothermal cure diagram for the epoxy-rich system, showing gelation, vitrification, and iso-T_g (every 20°C from 0 to $T_{g\infty}$) contours.

system begins to level off at $T_{g\infty 1}$, corresponding to full conversion of amine, but then increases again and levels off at $T_{g\infty 2}$ at the full conversion of epoxy.

At gelation ($T_g = {}_{gel}T_g$), the viscosity becomes infinite, and any flow that needs to occur in processing must occur prior to gelation. If the relationship between viscosity and conversion is known, viscosity can be calculated as a function of time and temperature and isoviscosity curves can be included in the TTT diagram[2] as an aid for designing cure

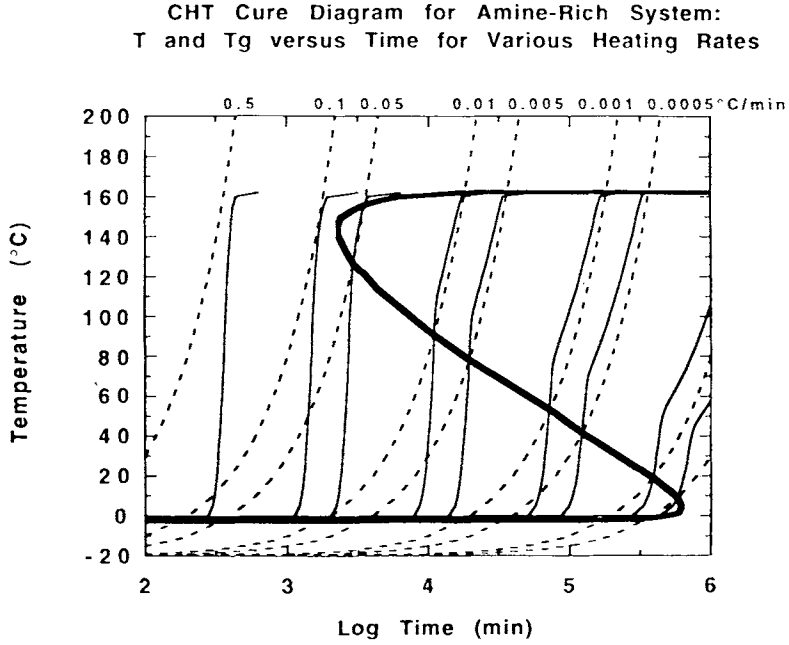

Figure 9 Calculated CHT cure diagram for the amine-rich system, showing the increase in cure temperature (dashed lines) and T_g (solid lines) vs. log time for various heating rates. The heavy line is the devitrification–vitrification–devitrification contour.

paths for processes in which flow is critical. The values of T_{g0} and ${}_{gel}T_g$ relative to room temperature are of primary practical importance. If T_{g0} < room temperature, the uncured sol mixture is a liquid at room temperature and can be used as a casting fluid. On the other hand, if room temperature < T_{g0}, then the uncured sol material is a glassy solid at room temperature and, on heating, will flow and react and can be used in molding technologies. Further, the shelf life (pot life) of the uncured material depends on the value of ${}_{gel}T_g$: If ${}_{gel}T_g$ > storage temperature, then even if the material reacts and solidifies during storage, it will remain sol and will flow upon heating and is still processable; however, if ${}_{gel}T_g$ < storage temperature, then the material will gel before it solidifies and the resulting sol/gel mixture is useless (e.g., it cannot be removed by flow from its container).

Calculation of Continuous-Heating-Transformation (CHT) Cure Diagram

Figures 9 and 10 show the calculated CHT cure diagrams for the two off-stoichiometric systems. To obtain the diagram, the rate constants in eqs. (3) and (4) are assumed to be Arrhenius and the change in temperature with time is added to the system of equations:

$$\frac{dx}{dt} = A_1 e^{-E_1/RT}(1 - x)(x + b)(1 - x_1 + \alpha x_2) + A_3 e^{-E_3/RT}(1 - x)x \quad (9)$$

$$\frac{dx_1}{dt} = A_1 e^{-E_1/RT} r(1 - x)(x + b)(1 - x_1) \quad (10)$$

$$\frac{dT}{dt} = m \quad (11)$$

where E and A are the activation energies and pre-exponential factors for the rate constants and m is the constant heating rate. These equations, along with eqs. (5)–(7), which account for diffusion control, and eq. (8), which relates T_g to conversion, are numerically integrated to yield conversion, T_g, and temperature as a function of time of reaction. The initial conditions for the integration were zero conversion and a temperature of −20°C. If the initial temperature is above T_{g0}, different results will be obtained. To obtain the CHT diagram, T_g and temperature are plotted vs. reaction time for various heating rates. The devitrification/vitrification/devitrification contour, which is the heavy solid contour in Figure 9 and Figure 10, is obtained by connecting the points where the T_g and temperature contours cross (i.e., where $T_g = T_c$). To the left of

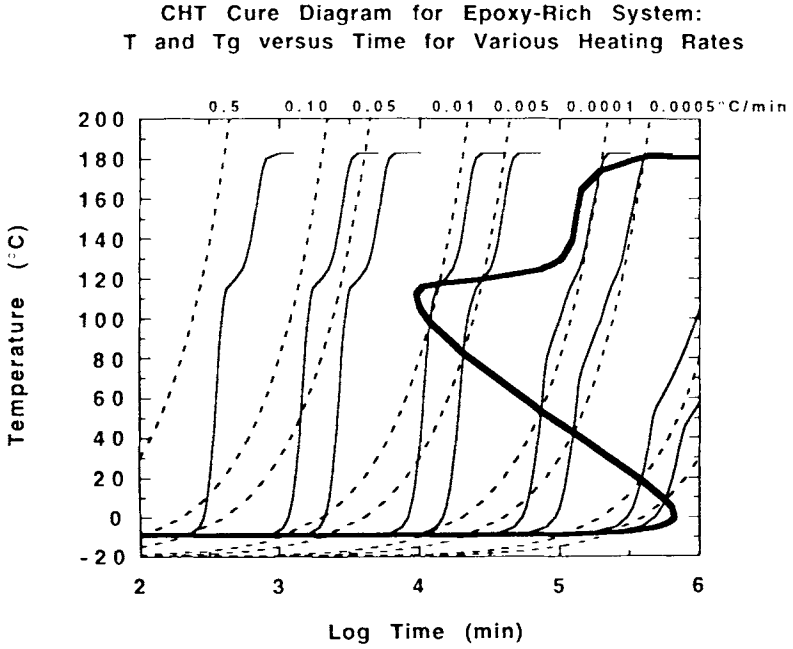

Figure 10 Calculated CHT cure diagram for the epoxy-rich system, showing the increase in cure temperature (dashed lines) and T_g (solid lines) vs. log time for various heating rates. The heavy line is a contour that includes devitrification and vitrification.

the contour, $T_g < T_c$ for each heating rate and the material is curing in the liquid, rubber, or glass transition region above T_g; to the right of the contour, $T_g > T_c$ for each heating rate and the material is curing in the glassy state or in the glass transition region below T_g. The devitrification–vitrification–devitrification contours are different shapes for the two off-stoichiometric systems, as might be expected. The contour in the amine-rich system is the typical S-shaped contour, with initial devitrification occurring in the lower portion of the curve, vitrification occurring in the intermediate region, and final devitrification occurring in the upper portion. In the epoxy-rich system, the etherification reaction complicates matters. In this case, the five segments of the curve represent initial devitrification, vitrification, devitrification, vitrification, and final devitrification. Another difference in the two systems is that, at the fastest heating rates shown, the epoxy-rich system does not reach full cure until the cure temperature is well above 250°C where thermal degradation reactions may occur. In practice, a ramp/hold cure should be used, with the hold at temperatures below those at which thermal degradation occurs but in the vicinity of $T_{g\infty}$ (see later).

The CHT diagrams show that for heating rates higher than an upper limiting value ($\gtrsim$ 0.07 and 0.02°C/min for the amine-rich and epoxy-rich systems, respectively), the average rate of increase of T_g is lower than the heating rate for all conversions so that the reaction is always kinetically controlled (i.e., $T_g < T_c$ throughout cure even though the instantaneous rate of increase of T_g may be greater than the heating rate at a particular conversion). Conversely, for very low heating rates (< 0.00004°C/min for both systems), the rate of increase of T_g is limited by the heating rate such that $T_g > T_c$ throughout cure and the reaction is always diffusion-controlled. Between these limiting heating rates, the amine-rich material will react initially in the liquid state ($T_g < T_c$), then it will vitrify as T_g catches up to T_c and react in the diffusion-controlled regime ($T_g > T_c$), and then as the reaction slows due to depletion of the reactants at high conversions, T_g will fall behind T_c and the material will devitrify and finish curing with $T_g < T_c$. Similarly, in the epoxy-rich system, the material may vitrify during the epoxy/amine reactions and then devitrify and cure in the rubbery state during the etherification reaction, or at lower heating rates, the material will vitrify during the epoxy/amine reactions and will not devitrify until high conversions after the etherification reaction is almost completed.

The two limiting regimes in the CHT diagram are important. For rapid curing operations, the reaction should be in the kinetically controlled regime throughout cure, and the material must be heated more rapidly than the upper limiting heating rate value. Conversely, curing in the glass transition region below T_g using the lower limiting value of the heating rate will yield material with maximum density and minimum internal stress due to the fact that no change of state will occur during curing and because the rate of physical aging (densification toward physical equilibrium) is greatest just below T_g. Note that the final T_c must be less than $T_{g\infty}$ so that $T_g > T_c$ throughout and after cure in order to retain the maximum density.[5]

DISCUSSION

Processing applications of the TTT and CHT diagrams that exploit or depend on gelation and/or vitrification will be discussed further below. Some of these examples may not be applicable to the present thermoset system, but are included to demonstrate and expound upon the concepts presented.

Processing to Achieve Full Conversion

Full conversion of a thermosetting material that reacts via a step-growth mechanism, such as the systems studied in this work, can be obtained by curing (or postcuring) only in the vicinity of or above $T_{g\infty}$ since the reaction rate generally decreases several orders of magnitude as the material vitrifies, generally over a region of $T_g = T_c \pm 20$ to 40°C. To achieve full conversion in the shortest time, a material must be reacted in the liquid state or after gelation in the sol/gel rubber state. Curing (or postcuring) at cure temperatures $\geq T_{g\infty} + 20$ to 40°C will generally ensure that full conversion is reached in a practical time for high-T_g systems, assuming that thermal degradation reactions are not significant at these relatively high reaction temperatures. If thermal degradation reactions do complicate the cure, a cure/postcure sequence is advisable to reduce the time at the higher reaction temperatures, although in some cases, especially with very highly cross-linked systems (i.e., high $T_{g\infty}$), full cure without thermal degradation may never be realized in practice. In the amine-rich system studied, full cure can be achieved for cure temperatures of $T_{g\infty} + 20$°C = 180°C in reasonable times ($\approx$ 100 min), whereas in the epoxy-rich system, full cure is impossible to

achieve in comparable times due to the slow rate of the etherification reactions coupled with the presence of thermal degradation reactions. The minimum time to obtain fractional conversions greater than 0.99 in the epoxy-rich system is 5000 min at $T_c = T_{g\infty 2} + 20°C = 200°C$, assuming thermal degradation does not occur.

Application to Cure of Large Parts

When curing large structures, such as an aircraft wing, the exothermic reaction will cause increased reaction rates and even degradation reactions if the rate of heat production (exotherm) is greater than the rate of heat dissipation. Inferior mechanical properties may result. Furthermore, the temperature gradients caused by large exotherms, with the center of the part generally being hotter than the exterior, may result in voids and stresses. Depending on the cure temperature (oven temperature), the temperature gradients will result in the inside or the outside of the part vitrifying first, as shown in Figure 11: If the cure temperature is below the cure temperature at which the time to vitrification is a minimum, the hotter interior will vitrify first; whereas if the cure temperature is above the cure temperature at which the time to vitrification is a minimum, the cooler exterior will vitrify first. The latter condition, where the exterior vitrifies prior to the interior, will result in greater internal stresses in the final part since contraction of the interior will be constrained by the fixed outer dimensions. The thermal stresses can be relieved by heating to above $T_{g\infty}$, although, subsequently, a slow cooling rate through T_g must be used to minimize temperature gradients that will again result in the cooler exterior vitrifying first.

To control the reaction rate and thus the exotherm and temperature gradients, the material can be step-cured at low and then higher temperatures, as is typical in composites manufacturing. An optimum step-cure cycle in which the reaction rate is less than a prespecified value can easily be determined from the TTT isothermal cure diagram in which the reaction rate is depicted by the horizontal distance between isoconversion contours at any particular cure temperature with the x-axis being linear time rather than log time. The closer together the isoconversion contours are, the higher the rate of reaction.

For the epoxy/amine system investigated, the reaction is autocatalyzed. Consequently, the maximum rate of reaction during isothermal cure occurs at an intermediate conversion, and the initial reaction rate is relatively slow. Similarly, the final rate of reaction is slow due to the depletion of reactants.

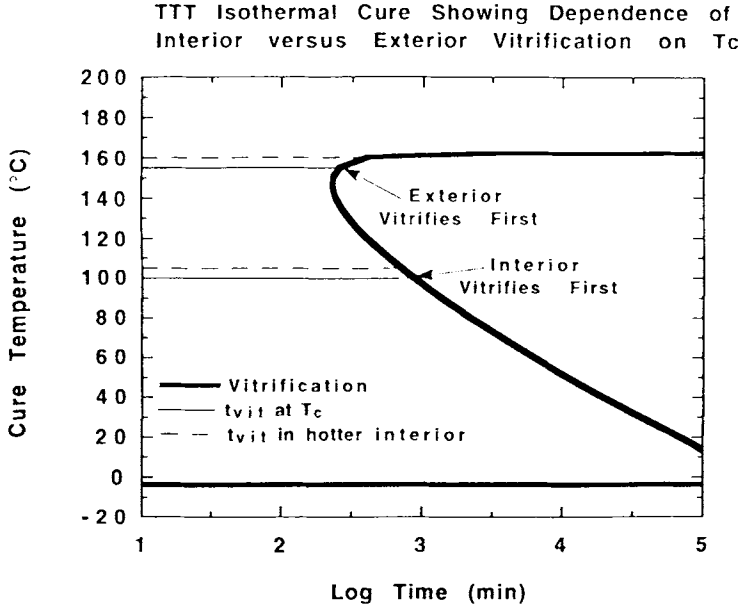

Figure 11 Calculated TTT isothermal cure diagram for the amine-rich system, showing the sequence of vitrification in the interior and exterior of the part vs. cure temperature. The solid line designates the time to vitrify at the cure temperature (oven temperature); the dashed line designates the time to vitrify in the hotter interior of the material.

Consequently, a reaction path for controlling the exotherm can be determined from the TTT isothermal cure diagram by keeping the isoconversion contours at least a prespecified interval apart. Such a path is diagrammed in Figure 12 for cure with $dx/dt \leq 0.003$ min^{-1}: 7.7 h at 100°C, 0.7 h at 120°C, 0.6 h at 130°C, 0.8 h at 140°C, and 0.9 h at 200°C. The same degree of cure with $dx/dt \leq 0.003$ min^{-1} can be obtained in a shorter time if cooling can be incorporated into the cure sequence. Initially, the reaction rate is slow (since the reaction is autocatalytic), and the initial cure temperature can be higher than 100°C while still keeping $dx/dt \leq 0.003$. For example, the first cure step could be replaced by cure at 115°C for 1.2 h and 100°C for 4.5 h, reducing the total cure time by 20%. Note that the rate of heat production by the step-cure method is much less than that for a straight isothermal cure at temperatures above $T_{g\infty}$: The reaction rate of 0.003 min^{-1} is much lower than the maximum rate observed during a straight isothermal cure at 200°C of 0.1 min^{-1}.

The rate of the exothermic reaction can also be controlled by curing at cure temperatures where the time scale of diffusion is comparable or greater than the time scale for the kinetically controlled reaction so that the reaction rate will be limited by the rate of diffusion. This method of controlling the exotherm requires no knowledge of the reaction kinetics and is inherently safe since the reaction is self-retarding in the diffusion-controlled regime (i.e., there is no possibility for a runaway reaction). For the present systems, the onset of diffusion control occurs approximately at vitrification. Consequently, to control the reaction rate, the material can be cured such that the cure temperature is always just below glass transition temperature of the material by using, e.g., a slow continuous heating rate (at or below the lower limiting rate in the CHT diagram). The cure of 250 gallons of initially liquid epoxy encapsulating a magnetic coil in the experimental Tokomak Fusion Test Reactor (TFTR) at Princeton University was accomplished by heating at a slow rate such that T_g increased in concert with the cure temperature.[1] An additional advantage of curing in the glass transition region below T_g is that the material will retain its shape during cure, although its dimensions will change (see later).

Cure and Design of Powder Coating Materials

For fluidized bed powder coating operations using thermosetting materials, a heated part can be dipped in a fluidized bed of the cool powder. The powder sticks to the part, and then upon subsequent heating, flows and cures to form a uniform coating. Thermosetting powder coatings can also be applied electrostatically using a spraygun; if the powder is ap-

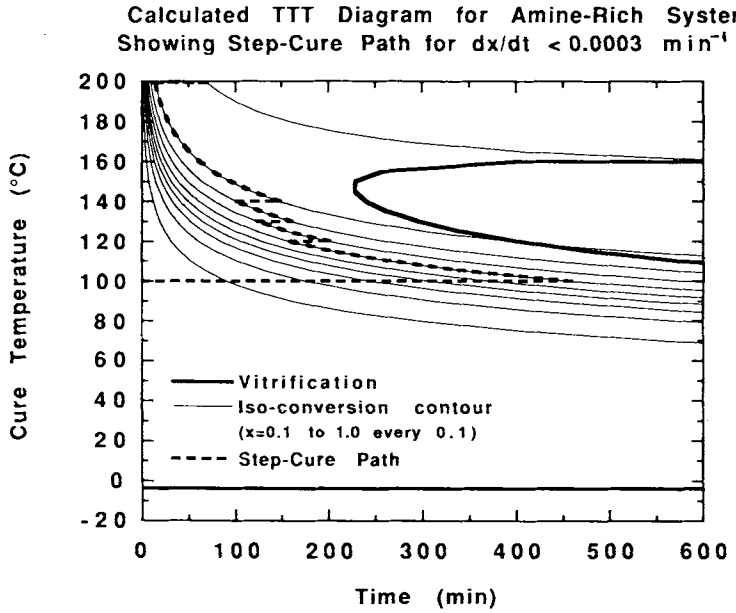

Figure 12 Calculated TTT isothermal cure diagram for the amine-rich system with a linear time axis showing vitrification and isoconversion (every 0.1 from $x = 0.0$–1.0) contours. A step-cure path is diagrammed to control the reaction rate at $dx/dt \leq 0.003$ min^{-1}.

plied to a cold charged part, it will stick to the part electrostatically and then flow and cure upon subsequent heating. The powder can also be electrostatically applied to a heated charged part; in this case, the powder may flow and react upon contacting the heated part, and the extra cure step may not be necessary. Regardless of the method of deposition, flow stops when the material gels as cure progresses. A postcure operation is often employed to obtain full conversion.

Powder coating formulations are generally made from low molecular weight reactants that have low viscosities and good flow characteristics. The T_g of the powder, T_{gi}, must be above room temperature (RT) but below ${}_{gel}T_g$. Thus, the material will be in the glassy state at room temperature (the powder will not be tacky). Since the powder coating material has not yet gelled ($T_g < {}_{gel}T_g$), it will be able to flow upon heating. Note that if it did not flow upon heating ($T_g > {}_{gel}T_g$), a poor coating would result.

In principle, another approach to designing thermoset powder coatings is to prereact a system whose T_g is initially below room temperature to produce a partially cured material with RT $< T_{gi} < {}_{gel}T_g$.[32] The time/temperature path to reach to produce such a material (with $T_g = T_{gi}$) can be calculated using the model of the curing reaction for the unreacted material. For isothermal cures, the time to reach the T_{gi} can also be simply read off the TTT diagram for the unreacted material (which can be calculated from the reaction model as in Figures 7 and 8 or can alternatively be determined experimentally for different systems where the reaction model is unknown). The utility of this approach to designing powder coatings will depend on whether the viscosity of the prereacted system is low enough to achieve flow and a uniform coating during cure. This will depend, of course, on the cure temperature and on the time to gelation at the cure temperature, which are inversely related. The advantage of this approach is the potential for using resin systems not originally formulated for powder coating operations.

New TTT isothermal cure diagrams for the powder coating material can be calculated from the reaction model starting from the initial T_g value T_{gi}, and these diagrams can be used to design the cure/postcure histories for obtaining full conversion. Figures 13 and 14 show the TTT diagrams calculated from the reaction model for amine-rich and epoxy-rich powder coating materials with initial fractional conversions of 0.50, corresponding to $T_{gi} \approx 42°C$ for both systems. (Recall that gelation would theoretically occur in the absence of intramolecular reactions[31] at fractional conversions of 0.65 and 0.53 for the epoxy-rich and amine-rich systems, respectively.) The times to reach specific conversions or vitrification are much reduced at lower isothermal curing temperatures compared to the uncured ma-

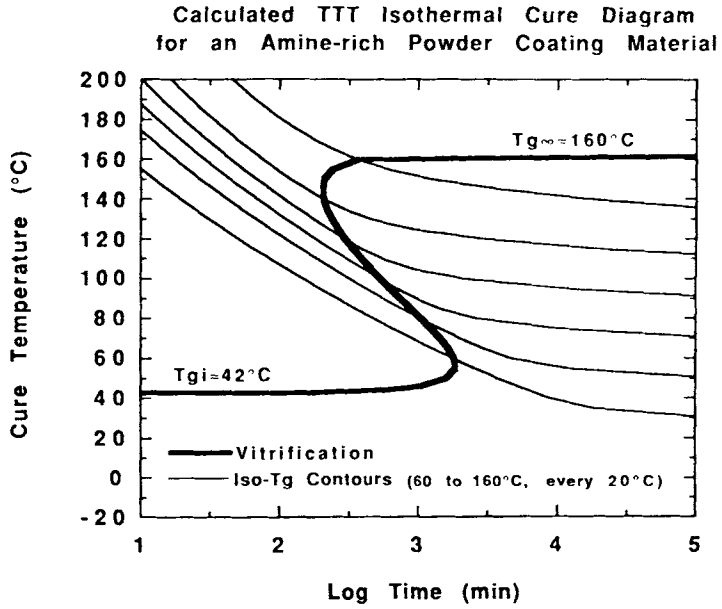

Figure 13 Calculated TTT isothermal cure diagram for an amine-rich powder coating material with $T_{gi} \approx 42$, showing vitrification and iso-T_g (every 20°C from 60 to 160°C) contours.

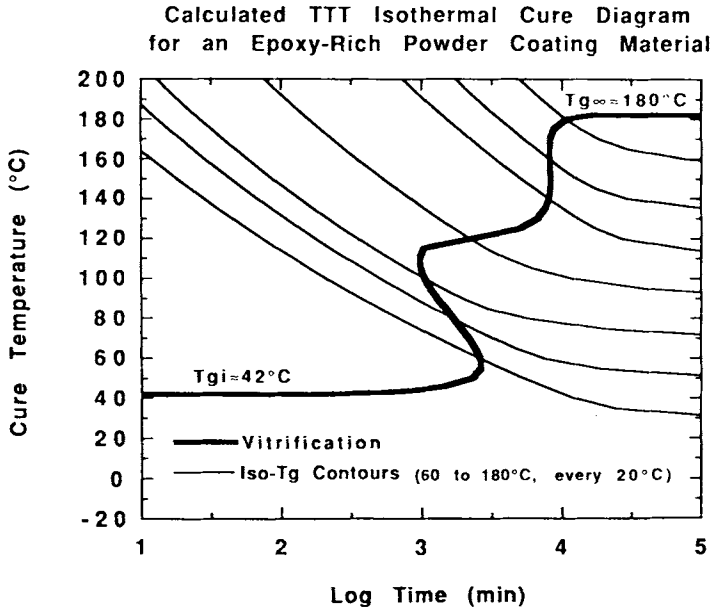

Figure 14 Calculated TTT isothermal cure diagram for an epoxy-rich powder coating material with $T_{gi} \approx 42$, showing vitrification and iso-T_g (every 20°C from 60 to 180°C) contours.

terial, as expected. However, the vitrification curves at relatively high cure temperatures (i.e., in the vicinity of $T_{g\infty}$) are not significantly altered since the time to vitrify is much greater than the time to reach T_{gi} at these cure temperatures.

For a cure/postcure sequence used for thermosetting powder coating materials, the time to reach a specific T_g at the cure temperature T_c and the time to reach $T_{g\infty}$ at the postcure temperature T_p can be determined from the TTT diagram. The cure time to reach a specific T_g at the cure temperature (t_{T_c}) can simply be read off the TTT diagram for the powder coating material (Figs. 13 and 14) or can alternatively be determined from the TTT diagram for the initially uncured reactants (Figs. 7 and 8) by subtracting the time to reach the initial T_g of the powder at the cure temperature (t_{T_{gi},T_c}) from the time to reach the desired T_g at the cure temperature (t_{T_g,T_c}):

$$t_{T_c} = t_{T_g,T_c} - t_{T_{gi},T_c} \tag{12}$$

This methodology only assumes that $T_c > T_{gi}$ (i.e., that the reaction of uncured material would be kinetically controlled prior to $T_g = T_{gi}$ at T_c). In fact, the reaction is generally kinetically controlled throughout cure with $T_c > T_g$ in order to minimize the time of cure. Similarly, the time to reach full conversion at the postcure temperature is found from the TTT diagram by subtracting the time to reach the starting T_g at the postcure temperature (t_{T_g,T_p}) from the time to reach $T_{g\infty}$ at the postcure temperature ($t_{T_{g\infty},T_p}$):

$$t_{T_p} = t_{T_{g\infty},T_p} - t_{T_g,T_p} \tag{13}$$

where it is assumed only that the postcure temperature $T_p > T_g$. Generally, the postcure temperature T_p should be greater than $T_{g\infty}$ to assure reaching full conversion in reasonable cure times but T_p should be lower than temperatures at which thermal degradation occurs. A similar methodology can be used to determine the time of step-cures.

Prepreg Design

Prepregs are fabrics used in composite manufacturing that are impregnated with liquid or solvent-bourne resins in a coating operation. The prepreg material is generally partially cured in order to achieve the desired tack characteristics at room temperature. Several layers of prepreg are stacked in a contoured assembly that is then cured to yield a fiber-reinforced composite laminate. For layups at room temperature, the glass transition temperature of the prepreg material, T_{gi}, should be slightly below room temperature so that the material is in the glass transition region at room temperature: If the T_g's of

the prepreg material were well above room temperature, the material would be a glass at room temperature and there would be no appreciable tack and shaping ability; whereas if it were well below room temperature, the material would be a liquid at room temperature and the prepreg would not be suitable for dry layups. The T_g of the prepreg, T_{gi}, should also be above the typical freezer storage temperature to ensure good shelf life with no significant reaction occurring during storage.

The time/temperature path to reach the desired T_g of the prepreg, T_{gi}, can be calculated using the model of the curing reaction for the unreacted material. For isothermal cures, the time to reach the T_{gi} can also be simply read off from the TTT diagram for the unreacted material.

A new TTT isothermal cure diagram for the prepreg material can be calculated from the reaction model, similar to the TTT diagrams for the powder coating materials. However, the time to reach T_g at any cure temperature above T_{gi} can also be determined from the original TTT diagram for the unreacted thermoset by subtracting the time to reach T_{gi} from the time to reach T_g at the specific cure temperature as described above for powder coating materials. Note that if solvent is used during the prepreg coating operation the solvent should be removed prior to gelation (see later).

Composite Processing

High-performance composite parts are generally cured in a mold at relatively high cure temperatures in an autoclave (pressurized oven) under moderate pressures for several hours and then postcured under atmospheric pressure to obtain full conversion. However, the autoclave process and the autoclave itself are expensive, and alternative processing techniques are preferable. The rapid thermoset cure (RTP) concept has recently been introduced to significantly reduce the autoclave cure time, thus reducing processing costs without any reduction of mechanical properties.[33] In the process, consolidation of the composite (fiber wetting, compaction, and air removal) occurs in the mold during the initial stages of cure at a temperature where the resin viscosity is initially low ($T_c \gg T_g$). Consolidation generally is accomplished with autoclave pressure although process costs can be substantially reduced if the autoclave is eliminated and vacuum pressure is used for consolidation. After consolidation, the composite material is cooled to below T_g (cooling is unnecessary if consolidation is accomplished at room temperature and T_g rises above room temperature as the cure/consolidation occurs). The material is then removed from the mold and postcured freestanding in a conventional oven such that the dimensional stability of the part is maintained by always curing in the glass transition region below T_g (i.e., $T_g \geq T_c$). Since T_g will increase during the postcure from the value after the cure step (T_{gi}) to the fully cured value, $T_{g\infty}$, the postcure should be a continuous heating ramp or ramp/hold sequence so that the postcure temperature is just below T_g in order to minimize the time of postcure while still maintaining the shape. The fastest rate of a continuous heating ramp at which $T_g > T_c$ throughout cure for a particular material with an initial T_g of T_{gi} is the rate at which vitrification occurs at T_{gi} in the CHT diagram. Note that the higher T_{gi}, the higher the heating rate can be. For example, for the amine-rich system, the maximum heating rates will be 0.01 and 0.05°C/min for values of T_{gi} of 90 and 130°C, respectively. The final curing temperature should be just below $T_{g\infty}$ so that the material will reach full conversion but will not devitrify (i.e., soften and possibly change shape under gravity or load).

Reaction Injection/Transfer Molding

Thermosetting resins are used as reaction injection-molding materials, e.g., to package electronic components. It is noted that these materials are generally much more reactive than are the systems studied in this work. Several criteria exist for designing the reaction injection-molding process for thermosetting materials. The process, itself, is relatively fast: Low viscosity material is injected into a hot mold, cured quickly, and then ejected solidified ($T_c < T_g$) at the cure temperature to retain dimensional stability and also to minimize time in the mold. The high molding temperatures used for fast reaction cause the viscosity of the material to increase rapidly during filling. It is critical that the mold be filled while the material is still liquid, i.e., prior to gelation. There is generally only a small window of cure temperatures for which gelation occurs after the mold is filled and vitrification occurs in a short time. The cure temperature should ideally be the temperature at which the time to vitrify is a minimum in order to minimize mold time provided that the gel time at this temperature is sufficiently long; this temperature is easily determined from the TTT diagram. Once the material has vitrified, it can be removed from the mold at the cure temperature and postcured free-standing to achieve full conversion. The post-

curing process must be accomplished such that the shape retention of the part is maintained by postcuring only in the glassy state or glass transition region below T_g. Since T_g will increase during the postcure from the initial value after curing to $T_{g\infty}$, the postcure should be a ramp/hold sequence so that the postcure temperature is just below T_g in order to minimize the time of postcure while maintaining the shape.

Cure of Solvent–Bourne Systems

The presence of solvent in solvent–bourne systems complicates the processing: If the solvent is not fully removed in the early stages of cure, the integrity of the final product is compromised by plasticization of the low molecular weight solvent and/or by the formation of voids from solvent evaporation at the high cure temperatures during the later stages of cure. The removal of solvent is limited by its diffusion out of the material, which is high when the material is in the liquid state, decreases through gelation, and is zero for all practical purposes once the material has vitrified.[30] To ensure removal of all solvent, the material should be step-cured, with the first step being at a temperature that allows adequate time for solvent removal prior to gelation. The material can then be fully cured at temperatures in the vicinity or above $T_{g\infty}$.

Cure of Rubber-modified Systems

The morphology of cured rubber-modified systems refers to the degree of phase separation and the size and distribution of the rubber-rich phase and depends on the cure history for systems that are initially homogeneous.[34–37] Rubber-rich particles phase separate from the thermoset-rich phase prior to gelation as cure progresses. The morphology depends on the thermodynamics (i.e., the temperature-dependent equilibrium phase separation) and on two kinetic time scales, the time scale for diffusion and aggregation of the rubber molecules and the time scale for gelation, both of which are controlled primarily by the cure temperature in the liquid state. The time scale for gelation is important, because once the material gels, the rate of aggregation decreases substantially.[35,37] The maximum degree of phase separation will generally occur at intermediate temperatures. At high cure temperatures, where the gel time is low, no phase separation is observed in a rubber-modified epoxy/amine system and the result is a plasticized optically homogeneous material.[34] Other work on rubber-modified epoxy/amine systems comparing catalyzed to uncatalyzed systems observed that the degree of phase separation decreased in the catalyzed system due to the relatively faster gel times.[37]

Controlling Final Properties

The final properties of a thermosetting material, including density, internal stresses, and modulus, are determined to a large extent by the processing. The maximum density for a specific fully cured material, which will also yield the minimum internal stress and maximum modulus, will be obtained by curing in the glass transition region below T_g throughout cure using a very slow temperature ramp from T_{g0} to $\leq T_{g\infty}$.[5] The maximum in modulus will be obtained by such a cure because the volume of the material below T_g is less than in the liquid state above T_g and because the rate of physical aging (spontaneous densification toward equilibrium) is a maximum just below T_g. The ramp rate below which the material always cures in the glassy state or glass transition region below T_g is inferred in the continuous-heating-transformation (CHT) cure diagram. However, such a temperature ramp is not feasible for processing the present system as it is too slow ($\leq$ 0.00004°C/min for the systems investigated), although it may be feasible for other systems.

The material properties can be manipulated further, however, by noting that the isothermal density after cure decreases with increasing conversion, as was observed in work on a high-T_g epoxy/amine system.[24] To this end, conversion–temperature–property diagrams are being developed in this laboratory that demonstrate the effect of conversion on the material properties of cured thermosetting systems.[38,39]

The aforementioned cure of 250 gallons of an initially liquid epoxy system to encapsulate and increase inertial give solid mass of an electromagnetic helical copper coil for the experimental Tokamak Fusion Test Reactor (TFTR) at the Princeton University Plasma Physics Laboratory (PPPL) is an example of the type of large scale engineering project which can be undertaken using thermosetting systems.[1] Although the encapsulated coils were constructed[40,41] without using the formal methodology of the present account, it is instructive to propose how to cure such a system in terms of the above account. A resin formulation would be selected to be fluid, nonvolatile, and relatively unreactive (to provide a long working life) at 25°C (e.g., T_{g0}

= −10°C), to gel at 25°C (e.g., ${}_{gel}T_g$ = 20°C) so as to minimize changes in shape on subsequent heating above 25°C, to be in the glassy state at the highest operating temperature (say 100°C), with $T_{g\infty}$ higher (at say 150°C) but not too high to preclude full cure without thermal degradation, and to fully react in a short time just above $T_{g\infty}$. T_{g0} is controlled by molecular weight, symmetry, and molecular flexibility of the constituents of the initial formulation. ${}_{gel}T_g$ and $T_{g\infty}$ can be adjusted by changing the functionality of reactants. Three successive stages of cure would be involved: 1) the liquid around the fiberglass-wrapped coil would be permitted to react at room temperature (25°C) in a mold for several days to form a glass, with T_g just above 25°C; 2) after loosening the mold the temperature would be raised very slowly over several more days to above $T_{g\infty}$ such that the rate of cure and the potential exotherm would be controlled during the further cure by the changing T_g being above the changing temperature of cure, which would also permit retention of the shape of the free-standing mass during heating; 3) the fully cured mass would be cooled very slowly to 25°C (so that the outside and inside would vitrify together and the effects of physical aging would be maximized) to form a glass at 25°C which would presumably have a lower density than that of the partially cured glass at 25°C (i.e., at the end of the first stage). The reason for loosening the mold after the initial stage of cure at 25°C would be to prevent the immense stresses which would otherwise have arisen in a contained system (within the mold) as a consequence of the net expansion at 25°C which arises from the increase in conversion, and from the thermal expansion and contraction which occur on heating and subsequent cooling. The procedure for making the first coil for the TFTR followed the proposed scheme in that an isothermal prereaction was followed by a temperature ramp reaction during which the mold was loosened. Subsequent coils were made using an elastomer between the coil and the hard mold, which in principle serves the same purpose as loosening the mold. More generally with respect to molding, the net expansion on converting a thermosetting material which has been partially cured to vitrify in a rigid mold to a fully cured material in the same mold could render it difficult, if not impossible, to remove the fully cured material from the mold.

CONCLUSIONS

A reaction model for the cure of a high-T_g epoxy/amine system, which includes etherification and diffusion-control, describes the experimental T_g vs. time DSC data for excess amine and excess epoxy systems using the one-to-one relationship between T_g and conversion. Two cure diagrams, the time–temperature–transformation (TTT) isothermal cure diagram and the continuous-heating-transformation (CHT) cure diagram, are calculated from the reaction model. The use of these cure diagrams for designing time/temperature cure programs for optimizing various processes or final material properties by exploiting gelation and/or vitrification is discussed.

REFERENCES

1. J. K. Gillham, *Polym. Eng. Sci.*, **26**(20), 1429 (1986).
2. J. B. Enns and J. K. Gillham, *J. Appl. Polym. Sci.*, **28**, 2567 (1983).
3. J. B. Enns and J. K. Gillham, in *Polymer Characterization*, ACS Adv. Chem. Ser. 203, C. D. Craver, Ed., American Chemical Society, Washington, DC, 1983, pp. 27–63.
4. L. C. Chan, H. N. Naé, and J. K. Gillham, *J. Appl. Polym. Sci.*, **41**, 1895 (1990).
5. G. K. Wisanrakkit and J. K. Gillham, *J. Appl. Polym. Sci.*, **42**, 2453 (1991).
6. G. K. Wisanrakkit and J. K. Gillham, *J. Appl. Polym. Sci.*, **41**, 2885 (1990).
7. X. Wang and J. K. Gillham, *J. Coat. Tech.*, **64**(807), 37 (1992).
8. S. L. Simon, PhD Thesis, Princeton University, January 1992.
9. S. L. Simon and J. K. Gillham, *J. Appl. Polym. Sci.*, **46**, 1245 (1992).
10. A. Hale, C. W. Macosko, and H. E. Bair, *Macromolecules*, **24**(9), 2610 (1991).
11. K. Horie, H. Hiura, M. Sawada, I. Mita, and H. Kambe, *J. Polym. Sci. A*, **18**, 1357 (1970).
12. L. Chiao, *Macromolecules*, **23**, 1286 (1990).
13. B. A. Rozenberg, *Adv. Polym. Sci.*, **78**, 113 (1986).
14. K. Dusek, *Adv. Polym. Sci.*, **78**, 1 (1986).
15. S. Lunak and K. Dusek, *J. Polym. Sci.*, **53**, 45 (1979).
16. A. C. Grillet, J. Galy, J. P. Pascault, and I. Bardin, *Polymer*, **30**, 2094 (1989).
17. X. Wang and J. K. Gillham, *J. Appl. Polym. Sci.*, **43**, 2267 (1991).
18. U. M. Bokare and K. S. Gandhi, *J. Polym. Sci. Polym. Chem.*, **18**, 857 (1980).
19. J. J. King and J. P. Bell, in *Epoxy Resin Chemistry*, ACS Symp. Ser. 114, R. S. Bauer, Ed., Washington, DC, 1979, pp. 225–257.
20. S. Matsuoka, X. Quan, H. E. Bair, and D. J. Boyle, *Macromolecules*, **22**, 4093 (1989).
21. W. M. Sanford and R. L. McCullough, *J. Polym. Sci. B Polym. Phys.*, **28**, 973 (1990).
22. A. K. Doolittle, *J. Appl. Phys.*, **22**, 1471 (1951).
23. M. L. Williams, R. F. Landel, and J. D. Ferry, *J. Am. Chem. Soc.*, **77**, 3701 (1955).

24. K. P. Pang and J. K. Gillham, *J. Appl. Polym. Sci.*, **37,** 1969 (1989).
25. J. Mijovic and J. Wijaya, *Macromolecules,* **23,** 3671 (1990).
26. C. Feger and W. J. MacKnight, *Macromolecules,* **18,** 280 (1985).
27. M. T. Aronhime and J. K. Gillham, *J. Coat. Tech.,* **56**(718), 35 (1984).
28. E. A. DiMarzio, *J. Res. Natl. Bur. Stds. A Phys. Chem.,* **68A,** 611 (1964).
29. D. R. Miller and C. W. Macosko, *Macromolecules,* **9**(2), 206 (1976).
30. S. Gan, J. K. Gillham, and R. B. Prime, *J. Appl. Polym. Sci.,* **37,** 803 (1989).
31. P. J. Flory, in *Principles of Polymer Chemistry,* Cornell University Press, Ithaca, NY, 1953.
32. S. L. Simon and J. K. Gillham, *J. Coat. Tech.,* **65,** 57 (1993).
33. W. V. Breitigam, R. S. Bauer, and C. A. May, *ACS Polym. Mat. Sci. Eng. Div. Prepr.* **66,** 511 (1992).
34. L. Chan, J. K. Gillham, A. J. Kinloch, and S. J. Shaw, in *Rubber Modified Thermosets,* Adv. Chem. Ser. 208, C. K. Riew and J. K. Gillham, Eds., American Chemical Society, Washington, DC, pp. 235–259.
35. L. T. Manzione, J. K. Gillham, and C. A. McPherson, *J. Appl. Polym. Sci.,* **26,** 889 (1981).
36. L. T. Manzione, J. K. Gillham, and C. A. McPherson, *J. Appl. Polym. Sci.,* **26,** 907 (1981).
37. J. K. Gillham, C. A. Glandt, and C. A. McPherson, in *Chemistry and Properties of Crosslinked Polymers,* S. S. Labana, Ed., Academic Press, New York, 1977, p. 291.
38. X. Wang and J. K. Gillham, *J. Appl. Polym. Sci.,* **47,** 425 (1993).
39. S. L. Simon and J. K. Gillham, *J. Appl. Polym. Sci.,* **51,** 1741 (1994).
40. J. C. McDade and L. E. Dudek, 9th Symposium on Engineering Problems of Fusion Research, IEEE Publication Number 81CH 1715-2NPS, Chicago, Illinois, October 26–29, 1981, Proceedings, Vol. 1, 335 (1981).
41. J. H. Chrzanowski, M. A. Pereira, and P. G. Snook, 9th Symposium on Engineering Problems of Fusion Research, IEEE Publication Number 81CH 1715-2NPS, Chicago, Illinois, October 26–29, 1981, Proceedings, Vol. 1, 339 (1981).

Received August 21, 1992
Accepted December 23, 1993